MULTIPLE SCLEROSIS JOURNAL | MSJ

Original Research Paper

Evidence of diffuse cerebellar neuroinflammation in multiple sclerosis by ^{11}C-PBR28 MR-PET

Multiple Sclerosis Journal

1–11

DOI: 10.1177/1352458519843048

Valeria T Barletta, Elena Herranz, Costantina A Treaba, Russell Ouellette, Ambica Mehndiratta, Marco Loggia, Eric C Klawiter, Carolina Ionete, Sloane A Jacob and Caterina Mainero

Abstract

Background: Activated microglia, which can be detected in vivo by ^{11}C-PBR28 positron emission tomography (PET), represent a main component of MS pathology in the brain. Their role in the cerebellum is still unexplored, although cerebellar involvement in MS is frequent and accounts for disability progression.

Objectives: We aimed at characterizing cerebellar neuroinflammation in MS patients compared to healthy subjects by combining ^{11}C-PBR28 MRI-Positron Emission Tomography (MR-PET) with 7 Tesla (T) MRI and assessing its relationship with brain neuroinflammation and clinical outcome measures.

Methods: Twenty-eight MS patients and 16 healthy controls underwent ^{11}C-PBR28 MR-PET to measure microglia activation in normal appearing cerebellum and lesions segmented from 7 T scans. Patients were evaluated using the Expanded Disability Status Scale and Symbol Digit Modalities Test. ^{11}C-PBR28 binding was assessed in regions of interest using 60–90 minutes standardized uptake values normalized by a pseudo-reference region in the brain normal appearing white matter. Multilinear regression was used to compare tracer uptake in MS and healthy controls and assess correlations with clinical scores.

Results: In all cerebellar regions examined, MS patients showed abnormally increased tracer uptake, which correlated with cognitive and neurological disability.

Conclusion: Neuroinflammation is widespread in the cerebellum of patients with MS and related to neurological disability and cognitive impairment.

Keywords: Cerebellum, neuroinflammation, MR-PET, microglia

Date received: 8 November 2018; revised: 5 March 2019; accepted: 8 March 2019

Correspondence to:
C Mainero
Athinoula A. Martinos Center for Biomedical Imaging, Department of Radiology, Massachusetts General Hospital, 149 13th Street, Charlestown, MA 02129, USA.
caterina@NMR.MGH.HARVARD.EDU

Valeria T Barletta
Elena Herranz
Costantina A Treaba
Marco Loggia
Caterina Mainero
Athinoula A. Martinos Center for Biomedical Imaging, Department of Radiology, Massachusetts General Hospital, Boston, MA, USA/Harvard Medical School, Boston, MA, USA

Russell Ouellette
Athinoula A. Martinos Center for Biomedical Imaging, Department of Radiology, Massachusetts General Hospital, Boston, MA, USA/Department of Clinical Neuroscience, Karolinska Institutet, Stockholm, Sweden

Ambica Mehndiratta
Athinoula A. Martinos Center for Biomedical Imaging, Department of Radiology, Massachusetts General Hospital, Boston, MA, USA

Eric C Klawiter
Department of Neurology, Massachusetts General Hospital, Boston, MA, USA/Harvard Medical School, Boston, MA, USA

Carolina Ionete
Multiple Sclerosis Center, UMass Memorial Medical Center, Worcester, MA, USA

Sloane A Jacob
Department of Neurology, Beth Israel Deaconess Medical Center, Boston, MA, USA/Harvard Medical School, Boston, MA, USA

Introduction

Cerebellar involvement occurs early in MS, where it contributes to disease progression and predicts poor outcome.[1,2] Neurological dysfunction related to cerebellar pathology in MS is generally highly disabling, since both motor and cognitive functions are affected.[3]

Cerebellar pathology in MS is characterized by extensive cortical and white matter (WM) demyelination, and neuronal loss.[3] In the MS brain, structural cortical and WM pathology closely associate with neuroinflammation.[4–7] Apart from scattered histological examinations in progressive disease that reported microglia activation in both the cerebellar WM and cortex,[8] the in vivo presence of neuroinflammation in the MS cerebellum is still to be characterized.

We combined ^{11}C-PBR28 imaging on an integrated 3 T MRI-Positron Emission Tomography (MR-PET) system with 7 Tesla (T) MRI to assess neuroinflammation in lesioned and normal appearing cerebellar tissue in patients at different stages of MS. ^{11}C-PBR28 is a second-generation radiotracer with high specificity and reproducibility that binds to the 18 kDa translocator protein (TSPO), which is overexpressed in activated microglia, a main component of neuroinflammation in MS.[9–11] Cerebellar lesions were

visualized on ultra-high resolution 7 T MRI, which demonstrated high sensitivity to focal lesion detection in MS.[12,13] We aimed at verifying the hypothesis that activated microglia represent a main component of cerebellar pathology in MS, and at investigating whether this activation is focal or diffuse, and whether it correlates with neuroinflammation in the brain. Finally, we investigated the association between cerebellar TSPO expression and clinical measures of neurological disability and information processing speed.

Materials and methods

Standard protocol approval, patient consents, and confidentiality

The Institutional Ethics Committee and the Radioactive Drug Research Committee approved all study procedures, and subjects gave written informed consent to participate in the study. Confidentiality of study subjects has been maintained through routine precautions: we assigned codes to identify the subjects, kept our records of procedures and scans in locked security cabinets. Only information necessary to conduct the study has been distributed to the study staff; all data stored in computers have been kept in a password-protected file, available only to investigators.

Subjects

Fourteen patients with relapsing–remitting multiple sclerosis (RRMS), 14 with secondary progressive multiple sclerosis (SPMS) and 16 age-matched healthy controls (HC), all with high- or mixed-affinity binding genotype for the TSPO gene,[14] were prospectively enrolled in the study. The study cohort overlaps (27/28 MS patients; 13/16 HC) with a previously published study assessing ^{11}C-PBR28 uptake in the brain.[15]

General inclusion criteria were age 18–65 years, education $\geqslant$8 years, absence of any treatment with benzodiazepines, no general PET and MRI contraindications, absence of major medical and/or psychiatric disorders (other than MS for patients). Inclusion criteria for MS were clinically definite MS,[16] absence of clinical relapse within 3 months, no corticosteroids therapy within 1 month of study enrollment, stable disease-modifying treatment, or no treatment for at least 6 months.

Clinical evaluation

Within 1 week from imaging procedures, all patients underwent neurological disability assessment through Expanded Disability Status Scale (EDSS).[17] Cognitive evaluation was performed using Symbol Digit Modalities Test (SDMT). SDMT raw scores were converted to Z-scores after correction for age and education.[18]

Imaging data acquisition

Patients and HC underwent ^{11}C-PBR28 MR-PET imaging on a Siemens (Erlangen, Germany) BrainPET system, a PET scanner operating in the bore of a 3 T whole-body MRI system equipped with an eight-channel head coil.[19] All subjects received an intravenous bolus injection of ^{11}C-PBR28, which was produced in house (mean $\pm$ SD administered dose = 11.4 ± 0.6 mCi in patients and 11.06 ± 0.8 mCi in HC, $p = 0.1$ by unpaired t-test), as previously detailed.[15] The PET data were acquired in list-mode format during a 90 minutes scan. Three-dimensional (3D) multi-echo magnetization prepared rapid acquisition gradient-echo (ME-MPRAGE) images (1 mm isotropic voxels) for attenuation correction,[20] co-registration of PET maps to 3 T data, FreeSurfer anatomical reconstruction for brain cortex and WM segmentation, and conventional 3D fluid-attenuated inversion recovery (FLAIR) images (1 mm isotropic voxels) for brain WM lesions segmentation, were simultaneously acquired to PET images. Patients also underwent 7 T MRI on a Siemens scanner using a 32-channel head coil, within ~1 week from the MR-PET session to acquire $0.6 \times 0.6 \times 1.5$ mm voxels T1-weighted Turbo-Fast Low-Angle Shot (TFL) images for cerebellar lesion segmentation. Three MS patients did not undergo 7 T imaging due to the presence of implants not approved for 7 T.

MRI and PET data analysis

Cerebellar lesions were segmented by consensus from two expert raters (V.T.B. and C.A.T.) on 7 T TFL images using a semiautomated method (3D Slicer v4.2.0) and defined as hypo-intensities extending at least three voxels across two consecutive slices.[21] In three MS patients that did not undergo 7 T imaging lesion segmentation was performed on ME-MPRAGE 3 T scans. Cerebellar lesions were classified as cortical (CL), leukocortical (LCL), white matter (WML), or deep grey matter (DGML). Lesion volume was computed using FSL version 5.0.7 (http://fsl.fmrib.ox.ac.uk/fsl/fslwiki/FSL). Masks of the whole cerebellum, cerebellar WM, and cortical grey matter (cGM) were segmented on 3 T T1-weighted images on ME-MPRAGE 3 T images using the automated software Volbrain (http://volbrain.upv.es).

Masks of cerebellar normal appearing white matter (NAWM) and cerebellar normal appearing cortical

grey matter (cNAGM) were obtained subtracting cerebellar lesion masks from the WM and cGM masks by FSL. To exclude that uptake in normal appearing tissue could be influenced by that in perilesional tissue, lesion masks were enlarged by 2 mm using FSL, and normalized tracer uptake values were extracted for NAWM and cNAGM before and after excluding perilesional areas. The subtracted NAWM and cNAGM masks were used in further analyses.

Brain WM lesions were segmented with 3D Slicer on FLAIR images. Brain WM and GM masks were segmented automatically by FreeSurfer on ME-MPRAGE images. Brain NAWM masks were obtained with FSL as for the cerebellum.

In-house software was used to compute voxel-wise standardized uptake values (SUV) (mean radioactivity/injected dose/weight) from the 60–90 minutes post-injection data (sampled at 1.25 mm isotropic voxel size) as previously detailed.[15] In each subject, the SUV map was normalized by a pseudo-reference region (SUVR) located in the brain NAWM, with mean SUV in MS patients around the mean of SUV in HC. As MS is a diffuse disease lacking an anatomically consistent reference region, the pseudo-reference region was identified by a cluster-based approach.[15] Using FSL and FreeSurfer tools, we identified clusters (minimum size 9 contiguous voxels) in the WM of HC and NAWM of patients that were within ± 0.5 SD of the mean ^{11}C-PBR28 SUV for the global WM in HC. This process was conducted separately for high- and mixed-affinity binders.[15] No differences were found in the clusters' SUV in patients versus HC (for high-affinity binders: mean SUV 0.71 ± 0.01 in patients vs 0.70 ± 0.01 in HC, $p = 0.3$; for mixed-affinity binders: mean SUV 0.54 ± 0.002 in patients vs 0.54 ± 0.002 in HC, $p = 0.1$ by multilinear regression covarying for age and gender).

Masks of normal appearing whole cerebellum, cerebellar NAWM and cNAGM, brain NAWM and GM, and lesions in both the brain and the cerebellum were registered to SUVR maps using FNIRT (FSL) to extract the mean SUVR. Lesions were grouped in WM lesions and cGM lesions to search for correlations with NAWM and cNAGM, respectively.

Statistical analysis

Statistical analysis was performed using JMP (https://www.jmp.com). Based on normality, Mann–Whitney test and Fisher's exact test were used to compare demographics and clinical characteristics in patients versus HC, and in RRMS versus SPMS. Multilinear regression models were used (1) to compare ^{11}C-PBR28 cerebellar uptake in patients versus HC in different regions of interest, (2) to correlate uptake in lesions and normal appearing tissue, (3) to search for associations between cerebellar uptake values and clinical metrics (disease duration, EDSS, SDMT), (4) to assess correlation between SUVR in the cerebellum and in the brain. Gender, binding affinity, age, and disease duration were included as covariates of no interest when appropriate. Matched-pairs *t*-test compared uptake in lesions and non-lesioned tissue in patients. A p value < 0.05 was considered statistically significant.

Results

Demographic and clinical characteristics

Demographic and clinical data of study subjects are shown in Table 1.

Patients and HC did not differ in age, gender, and binding affinity. No differences were found between the two MS sub-groups for gender and binding affinity. As expected, RRMS were younger ($p = 0.005$), had shorter disease duration ($p < 0.001$), and lower EDSS ($p < 0.001$) than SPMS patients. Cognitive scores were also lower in SPMS relative to RRMS cases ($p < 0.001$). One patient with RRMS was not able to complete the test because of important visual impairment. Twenty-two patients (12 RRMS and 10 SPMS) were on disease-modifying therapy.

Cerebellar lesions

Cerebellar lesions were found in the majority of MS patients: in 11/14 RRMS and 13/14 SPMS. In RRMS, most lesions were localized in the WM; in SPMS, lesions involved more frequently the cerebellar cortex, either intracortically or leukocortically. The detailed spatial localization of cerebellar lesions segmented at 7 T is shown in Table 2. Figure 1(a)–(d) illustrates a few examples of cerebellar lesions at 7 T. WML in the cerebellum typically involved the peduncles, and the hilar regions of the deep nuclei (Figure 1(b) and (d)); leukocortical lesions showed a broader extension in the WM and involved the cortex to smaller extent (Figure 1(a)); pure cortical lesions were seemingly confined within the folia (Figure 1(c)).

No cerebellar lesions were observed in HC.

Table 1. Demographic and clinical characteristics of study subjects.

Characteristic	HC ($n=16$)	All MS ($n=28$)	RRMS ($n=14$)	SPMS ($n=14$)
Age, mean (SD)	47 (12)	48 (10)	43 (9)	53 (7)
Gender, F/M	11/6	22/6	11/3	11/3
Affinity, high/mixed	8/8	15/13	7/7	8/6
Disease duration, median	–	9	2	21.5
EDSS, median (range)	–	3.5 (1.5–7.5)	2 (1.5–6)	6.5 (2.5–7.5)
SDMT Z-score, median	–	0.03	0.77	–1.4
MS treatment				
Dimethyl fumarate	–	7	5	2
Natalizumab	–	5	2	3
Glatiramer acetate	–	4	2	2
Rituximab	–	3	1	2
Interferon beta 1a	–	2	2	0
Fingolimod	–	1	0	1
None	–	6	2	4

HC: healthy controls; MS: multiple sclerosis; RRMS: relapsing–remitting multiple sclerosis; SPMS: secondary progressive multiple sclerosis; EDSS: Expanded Disability Status Scale; SDMT: Symbol Digit Modalities Test.

Table 2. Cerebellar lesion count and volume of according to their location and disease subtype.

	RRMS	SPMS
Cortical lesions		
Count, median (range)	1 (0–2)	2 (0–4)
Volume, mean ± SD (range)	$37 \pm 19\,mm^3$ (21–58)	$74 \pm 47\,mm^3$ (10–127)
Number of patients	3/14	6/14
Leukocortical lesions		
Count, median (range)	2 (0–3)	2.5 (0–9)
Volume, mean ± SD (range)	$108 \pm 39\,mm^3$ (70–166)	$187 \pm 222\,mm^3$ (17–791)
Number of patients	5/14	10/14
Deep grey matter lesions		
Count, median (range)	1 (0–1)	1 (0–2)
Volume, mean ± SD (range)	$77 \pm 63\,mm^3$ (43–205)	$198 \pm 201\,mm^3$ (17–525)
Number of patients	6/14	6/14
White matter lesions		
Count, median (range)	1 (0–4)	2 (0–6)
Volume, mean ± SD (range)	$154 \pm 168\,mm^3$ (27–521)	$98 \pm 127\,mm^3$ (10–340)
Number of patients	7/14	7/14

RRMS: relapsing–remitting multiple sclerosis; SPMS: secondary progressive multiple sclerosis; SD: standard deviation.

Tracer uptake in MS compared to HCs

The ^{11}C-PBR28 uptake was overall higher in patients relative to HC in all the cerebellar regions examined (Figure 2).

The highest ^{11}C-PBR28 SUVRs were found in cerebellar lesions (mean SUVR 1.43 ± 0.3), followed by the NAWM and cNAGM in patients (mean SUVR $= 1.42 \pm 0.3$ and 1.38 ± 0.3, respectively) and WM and GM in HC (mean SUVR $= 1.23 \pm 0.2$ and 1.20 ± 0.2, respectively). Figure 3 shows ^{11}C-PBR28 SUVR distribution across cerebellar regions in HC and MS subjects, according to their binding genotype.

When correcting for age, gender, and binding affinity, MS patients showed abnormally increased ^{11}C-PBR28 uptake in lesions compared to the HC's whole cerebellum ($p=0.03$), as well as in NAWM ($p=0.03$) and cNAGM ($p=0.04$) versus WM and cGM in HCs, respectively. As an outlier was present when

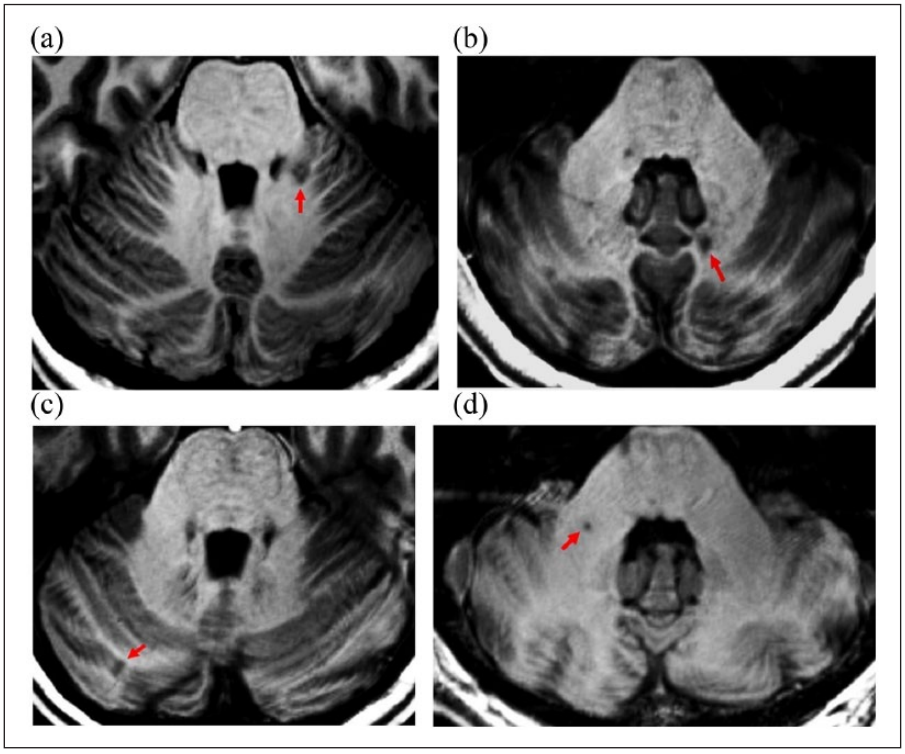

Figure 1. Cerebellar lesions on 7 T Turbo-Fast Low-Angle Shot images. Cerebellar lesions (arrows) in multiple sclerosis patients in different regions of interest: (a) leukocortical, (b) deep grey matter (left dentate), (c) cortical, and (d) white matter.

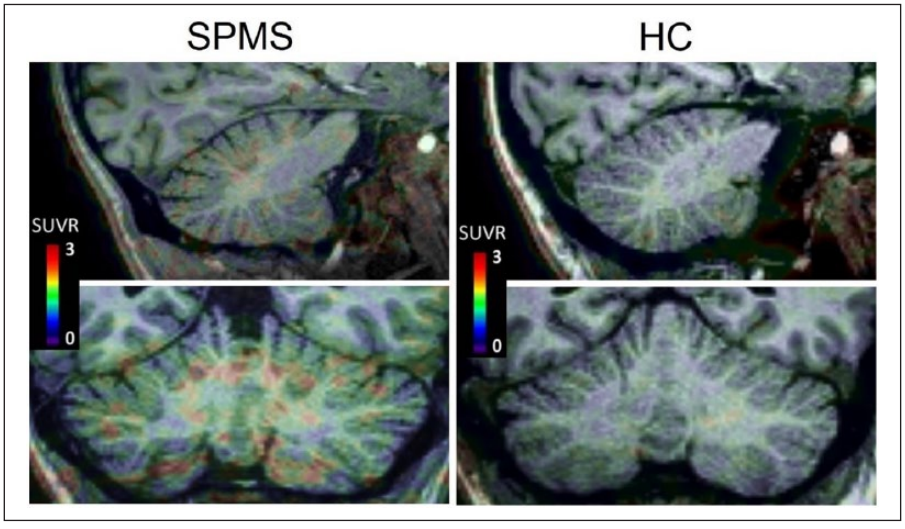

Figure 2. Fused MRI and PET images.
Images from a patient with progressive multiple sclerosis and a healthy subject, both mixed-affinity binders, showing overall higher uptake in the first.
SPMS: secondary progressive multiple sclerosis; HC: healthy control; SUVR: standardized uptake values normalized by a pseudo-reference region.

measuring lesion uptake in patients (Figure 3), the analysis was repeated after excluding that datum and the significant difference with HC's whole cerebellum uptake persisted ($p = 0.03$).

To assess whether increased TSPO expression in the cerebellar NAWM and cNAGM could be driven by inflammation in perilesional tissue, the analysis was repeated excluding the perilesional area. We found

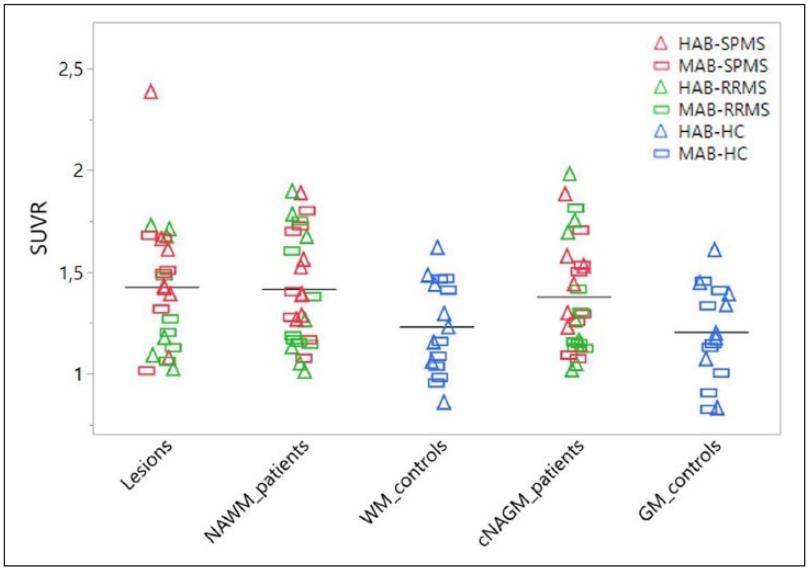

Figure 3. Mean ^{11}C-PBR28 standardized uptake values in MS patients and healthy controls.
Scatter plot showing individual mean ^{11}C-PBR28 standardized uptake values normalized by a pseudo-reference region (SUVR) in patients and healthy controls. Bars represent group means.
NAGM/GM: normal appearing grey matter/grey matter; NAWM/WM: normal appearing white matter/white matter; HC: healthy controls; MS: multiple sclerosis; RRMS: relapsing–remitting multiple sclerosis; SPMS: secondary progressive multiple sclerosis; HAB: high-affinity binders; MAB: mixed-affinity binders.

that NAWM and cNAGM SUVR were still higher in patients than in HC ($p=0.03$ and $p=0.04$, respectively).

Although cerebellar ^{11}C-PBR28 uptake was overall higher in SPMS relative to RRMS patients (NAWM: mean SUVR 1.46 ± 0.2 vs 1.37 ± 0.3; NAGM: mean SUVR 1.4 ± 0.2 vs 1.36 ± 0.3; lesions: mean SUVR 1.51 ± 0.3 vs 1.32 ± 0.3), these differences were not significant ($p=0.7$ for NAWM, $p=0.9$ for NAGM, $p=0.4$ for lesions by linear regression models after correcting for age, gender and binding affinity). We did not find differences in ^{11}C-PBR28 uptake in treated versus untreated patients in any region examined.

Finally, we investigated the relationship between tracer uptake in lesions and in corresponding normal appearing tissue. Tracer uptake in cGM lesions correlated with cNAGM SUVR (coefficient = 0.56; confidence interval (CI) = 0.35,0.78; $p < 0.0001$), although SUVR in lesions were higher than in cNAGM (mean SUVR 1.49 ± 0.4 vs 1.38 ± 0.3, $p=0.02$ by matched-pairs *t*-test). A modest correlation was seen between WM lesions and NAWM uptake (coefficient = 0.45; CI = 0.05,0.85; $p=0.03$), with no differences in the mean values (mean SUVR 1.37 ± 0.3 vs 1.42 ± 0.3, $p=0.4$ by *t*-test).

Correlation with brain uptake values

We found positive correlations between tracer uptake in the cerebellum and in the brain. In particular, we tested cerebellar NAWM versus brain NAWM uptake (coefficient = 1.05; CI = 0.83,1.27; $p < 0.0001$), cerebellar cGM versus brain cGM uptake (coefficient = 0.95; CI = 0.77,1.13; $p < 0.0001$), cerebellar lesions uptake versus brain WM lesions uptake (coefficient = 0–87; CI = 0.29,1.44; $p=0.005$) (Figure 4).

Correlations with clinical metrics

No correlation was found between tracer uptake and disease duration. Both EDSS and SDMT correlated with disease duration ($p < 0.001$ and $p=0.01$, respectively). There was a positive correlation between EDSS and SUVR in NAWM ($p=0.02$), cNAGM ($p=0.03$), and lesions ($p=0.02$). We also found a negative correlation between SDMT scores and SUVR in NAWM ($p=0.03$), but not in cNAGM or in lesions (see Table 3 for more details).

No correlations were found between tracer uptake and cerebellar subscores for NAWM ($p=0.2$), cNAGM ($p=0.1$), and lesions ($p=0.1$). Figure 5 illustrates the correlations between tracer uptake and clinical metrics.

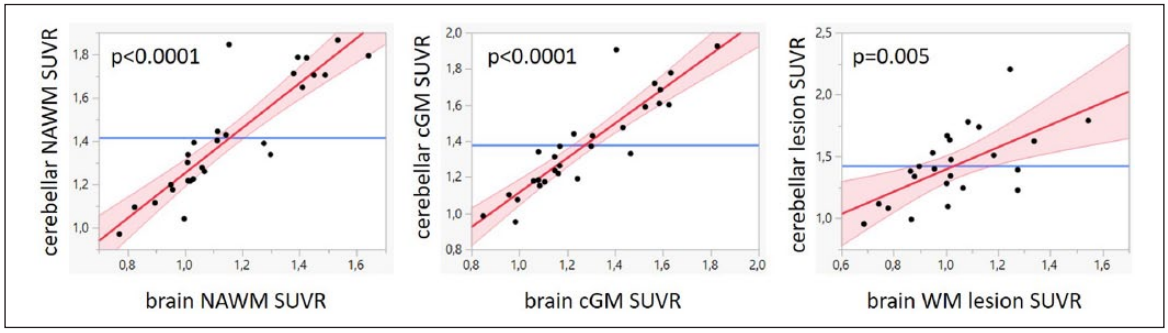

Figure 4. Scatter plots showing the correlation between cerebellar and brain SUVR.
NAWM: normal appearing white matter; SUVR: standardized uptake values normalized by a pseudo-reference region; cGM: cortical grey matter; WM: white matter.

Table 3. Linear correlations between clinical metrics and tracer uptake.

	Disease duration	NAWM SUVR	cNAGM SUVR	Lesion SUVR
EDSS				
Coefficient	0.12	1.77	2.15	1.77
CI	0.06, 0.18	0.35, 3.20	0.23, 4.06	0.35, 3.20
p value	< 0.001	0.02	0.03	0.02
SDMT				
Coefficient	–0.08	–2.42	–1.8	–1.45
CI	–015, –0.02	–0.64, –0.19	–4.12, 0.44	–3.60, 0.7
p value	0.01	0.03	0.1	0.2

EDSS: expanded disability status scale; SDMT: Symbol Digit Modalities Test; NAWM: normal appearing white matter; cNAGM: normal appearing cortical grey matter; SUVR: standardized uptake values normalized by a pseudo-reference region; CI: confidence interval.

Discussion

In this study, using ^{11}C-PBR28 MR-PET and 7 T MRI, we investigated the presence of neuroinflammation in the cerebellum of RRMS and SPMS cases. We found that relative to HC, patients had abnormally increased TSPO expression, a marker of microglia activation, in both lesioned and normal appearing cerebellar WM and cortex. Neuroinflammation correlated with decreased information processing speed and neurological disability.

Previous PET studies did not report increased TSPO expression in the cerebellum of MS patients.[6] This could be explained by the fact that previous data were obtained using ^{11}C-PK11195, which shows significantly lower binding specificity than ^{11}C-PBR28.[22]

Using 7 T MRI, we detected cerebellar lesions in the majority of patients. In RRMS, lesions were mainly located in the WM; in SPMS, there was a predominance of cortical and leukocortical plaques. Our findings are in line with previous reports on the presence and distribution of cerebellar lesions in the disease.[23] We segmented lesions on T1-weighted images because previous examinations demonstrated that 7 T T1 sequences have higher sensitivity than 3 T MRI to cerebellar lesions in MS, especially those located cortically and leukocortically.[13] Histopathology shows that demyelinated plaques can be widespread in the WM and GM of the cerebellum in MS, since the early phase of the disease. Demyelination seems to mainly involve the cerebellar cortex especially in the progressive phase; in some case, WM plaques could be undetectable even in the presence of extensive cortical demyelination.[24]

As we previously reported,[15] ^{11}C-PBR28 SUVR is a reliable method for characterizing microglial pathology in MS, since it has a strong positive correlation with the radiotracer volume of distribution. We also demonstrated that MS subjects and controls showed similar levels of ^{11}C-PBR28 plasma concentrations, and no differences in the area under the blood curves.[25]

In our MS cohort, abnormally increased TSPO signal extensively involved the WM, both lesions and normal appearing tissue. Microglia activation can be frequently detected in WM lesions and NAWM[7,26] in the brain of

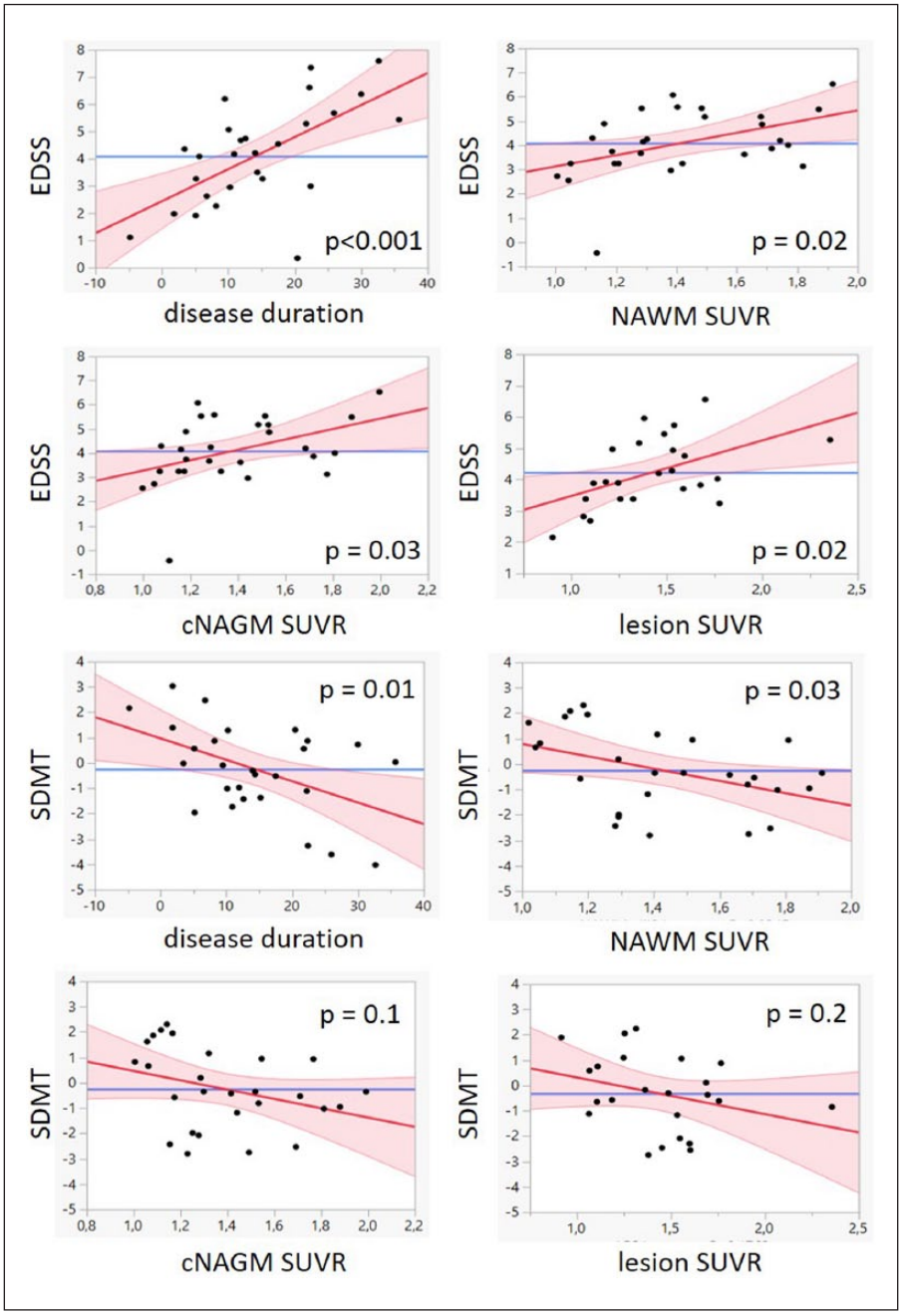

Figure 5. Scatter plots showing the correlation between tracer uptake and clinical metrics in MS patients.
EDSS: expanded disability status scale; NAWM: normal appearing white matter; SUVR: standardized uptake values normalized by a pseudo-reference region; cNAGM: normal appearing cortical grey matter; SDMT: symbol digit modalities test.

MS patients. Within lesioned tissue, inflammation is most severe in active and expanding lesions.[27]

In NAWM, activated microglia mainly features the progressive disease, while it is less pronounced in the relapsing phase.[6,7,26] We found similar results for cerebellar NAWM, where tracer uptake was higher in patients than in HC, especially in progressive MS. However, in our analysis, cerebellar deep nuclei were not segmented apart from the WM; thus, the SUVR in the WM was a combination of WM and deep GM uptake.

Interestingly, as observed previously for the MS brain,[15] we found that microglia activation also involved the cerebellar cortex, especially lesions and SPMS disease stages, indicating that neuroinflammation is a relevant component of cerebellar

cortical pathology in the disease. Ex vivo MS studies have suggested the presence of a link between cortical microglia activation, demyelination, and diffuse meningeal inflammation[8,24,26] Meningeal inflammation in the brain has been associated to the presence of aggregates of B-cells, organized in ectopic lymphoid follicle-like structures.[4] These structures seem to accompany a condition of higher cortical inflammation driven by activated microglia.[28] Although meningeal inflammation was pathologically found also in the cerebellum, evidence of follicle-like structures therein is still lacking.[8,24] Future studies are needed to clarify the role of meningeal inflammation and microglia activation in cerebellar cortical pathology and its relationship with overlying brain neuroinflammation.

In our study, cerebellar neuroinflammation was widespread throughout all the regions of interest, and not strictly influenced by perilesional uptake. In addition, ^{11}C-PBR28 uptake in the cerebellum strongly correlated with tracer uptake in the brain, suggesting that neuroinflammation in MS is diffuse to the whole CNS rather than restricted to the supra- or infratentorial compartments.

We previously found a positive correlation between EDSS and ^{11}C-PBR28 uptake values in the brain NAWM, thalamus and cortex.[15] This was seen also in the cerebellum, where tracer uptake diffusively correlated with EDSS. As known, cerebellar symptoms contribute to the overall EDSS score. Moreover, cerebellar structural abnormalities seem to correlate with EDSS, even in absence of clinical signs of cerebellar dysfunction,[29] and MS patients with cerebellar signs are known to have more severe disease with poor prognosis.[1,2]

We also found that lower SDMT scores correlated with increased TSPO expression in the NAWM, as previously demonstrated for the brain.[15] Cognitive impairment with information processing speed dysfunction frequently occurs in MS, as the result of damage affecting multiple areas, including the cerebellum.[3] Patients with motor cerebellar signs specifically showed decreased performance in attention and verbal fluency tasks,[30] and structural abnormalities in the MS cerebellum have been shown to correlate with SDMT scores and overall cognitive function.[31,32] Structural alterations in the WM can be responsible for interruption of the pathways connecting cerebellum and supratentorial structures, leading to motor and cognitive impairment. Moreover, diffusion tensor imaging analyses reported diffuse WM microstructural abnormalities in the cerebellum of MS subjects, compared to a more restricted, selective damage in the GM.[33]

There are a few limitations to our study. First, we cannot exclude that the small dimensions of some of the cerebellar lesions detected at 7 T might have impacted the accuracy of tracer quantification within lesions, although the effect should be mitigated in normal appearing tissue where perilesional tissue was excluded. However, the finding that ^{11}C-PBR28 uptake in cortical lesions was significantly higher than in cNAGM suggests that partial volume effects in lesion SUVR estimation may not be as relevant. Second, previous investigations have suggested that an endothelial binding component could affect ^{11}C-PBR28 tracer quantification.[34] Although this has not been definitively proven in MS, future studies will address this component for accurate tracer uptake estimation. Longitudinal investigations in larger MS cohorts are needed to better clarify the role of cerebellar glial activation in the progression of disease and in the occurrence of neurodegeneration.

Declaration of Conflicting Interests

The author(s) declared the following potential conflicts of interest with respect to the research, authorship, and/or publication of this article: C.I. has received research support from Genzyme/Sanofi, Biogen Idec, Genentech and financial compensations for scientific advisory from Genzyme/Sanofi. S.A.J. is a consultant on advisory boards for Biogen, Teva, Genentech, Celgene, Genzyme; has grant funding from Genzyme, Biogen. C. M. has received research support by Genzyme Sanofi and Serono Merck. Other authors declare no potential conflicts of interest.

Funding

The author(s) disclosed receipt of the following financial support for the research, authorship, and/or publication of this article: This study was supported by National Multiple Sclerosis Society (NMSS; RG 4729A2/1), the US Army, Department of Defense (W81XWH-13-1-0112), NIH (R01 NS078322-01-A1). E.H. was supported by NMSS fellowship (FG-1507-05459).

ORCID iD

Valeria T Barletta https://orcid.org/0000-0003-0655-9406

References

1. Amato MP and Ponziani G. A prospective study on the prognosis of multiple sclerosis. *Neurol Sci* 2000; 21: S831–S838.
2. Eriksson M, Andersen O and Runmarker B. Long-term follow up of patients with clinically isolated

syndromes, relapsing-remitting and secondary progressive multiple sclerosis. *Mult Scler* 2003; 9(3): 260–274.

3. Weier K, Banwell B, Cerasa A, et al. The role of the cerebellum in multiple sclerosis. *Cerebellum* 2015; 14: 364–374.
4. Magliozzi R, Howell O, Vora A, et al. Meningeal B-cell follicles in secondary progressive multiple sclerosis associate with early onset of disease and severe cortical pathology. *Brain* 2007; 130(Pt. 4): 1089–1104.
5. Howell OW, Reeves CA, Nicholas R, et al. Meningeal inflammation is widespread and linked to cortical pathology in multiple sclerosis. *Brain* 2011; 134(Pt. 9): 2755–2771.
6. Rissanen E, Tuisku J, Rokka J, et al. In vivo detection of diffuse inflammation in secondary progressive multiple sclerosis using PET imaging and the radioligand ^{11}C-PK11195. *J Nucl Med* 2014; 55(6): 939–944.
7. Giannetti P, Politis M, Su P, et al. Increased PK11195-PET binding in normal-appearing white matter in clinically isolated syndrome. *Brain* 2015; 138(Pt. 1): 110–119.
8. Howell OW, Schulz-Trieglaff EK, Carassiti D, et al. Extensive grey matter pathology in the cerebellum in multiple sclerosis is linked to inflammation in the subarachnoid space. *Neuropathol Appl Neurobiol* 2015; 41(6): 798–813.
9. Kreisl WC, Fujita M, Fujimura Y, et al. Comparison of [(11)C]-(R)-PK 11195 and [(11)C]PBR28, two radioligands for translocator protein (18 kDa) in human and monkey: Implications for positron emission tomographic imaging of this inflammation biomarker. *Neuroimage* 2010; 49: 2924–2932.
10. Park E, Gallezot JD, Delgadillo A, et al. (11) C-PBR28 imaging in multiple sclerosis patients and healthy controls: Test-retest reproducibility and focal visualization of active white matter areas. *Eur J Nucl Med Mol Imaging* 2015; 42(7): 1081–1092.
11. Moll NM, Rietsch AM, Thomas S, et al. Multiple sclerosis normal-appearing white matter: Pathology-imaging correlations. *Ann Neurol* 2011; 70(5): 764–773.
12. Filippi M, Evangelou N, Kangarlu A, et al. Ultra-high-field MR imaging in multiple sclerosis. *J Neurol Neurosurg Psychiatry* 2014; 85: 60–66.
13. Fartaria MJ, O'Brien K, Sorega A, et al. An ultra-high field study of cerebellar pathology in early relapsing-remitting multiple sclerosis using MP2RAGE. *Invest Radiol* 2017; 52(5): 265–273.
14. Owen DR, Yeo AJ, Gunn RN, et al. An 18-kDa translocator protein (TSPO) polymorphism explains differences in binding affinity of the PET radioligand PBR28. *J Cereb Blood Flow Metab* 2012; 32(1): 1–5.
15. Herranz E, Gianni C, Louapre C, et al. Neuroinflammatory component of gray matter pathology in multiple sclerosis. *Ann Neurol* 2016; 80(5): 776–790.
16. Polman CH, Reingold SC, Banwell B, et al. Diagnostic criteria for multiple sclerosis: 2010 revisions to the McDonald criteria. *Ann Neurol* 2011; 69(2): 292–302.
17. Kurtzke JF. Rating neurologic impairment in multiple sclerosis: An expanded disability status scale (EDSS). *Neurology* 1983; 33(11): 1444–1452.
18. Parmenter BA, Testa SM, Schretlen DJ, et al. The utility of regression-based norms in interpreting the minimal assessment of cognitive function in multiple sclerosis (MACFIMS). *J Int Neuropsychol Soc* 2010; 16(1): 6–16.
19. Kolb A, Wehrl HF, Hofmann M, et al. Technical performance evaluation of a human brain PET/MRI system. *Eur Radiol* 2012; 22(8): 1776–1788.
20. Izquierdo-Garcia D, Hansen AE, Forster S, et al. An SPM8-based approach for attenuation correction combining segmentation and nonrigid template formation: Application to simultaneous PET/MR brain imaging. *J Nucl Med* 2014; 55(11): 1825–1830.
21. Louapre C, Govindarajan ST, Gianni C, et al. Beyond focal cortical lesions in MS: An in vivo quantitative and spatial imaging study at 7T. *Neurology* 2015; 85(19): 1702–1709.
22. Hannestad J, Gallezot JD, Schafbauer T, et al. Endotoxin-induced systemic inflammation activates microglia: [^{11}C]PBR28 positron emission tomography in nonhuman primates. *Neuroimage* 2012; 63(1): 232–239.
23. Calabrese M, Mattisi I, Rinaldi F, et al. Magnetic resonance evidence of cerebellar cortical pathology in multiple sclerosis. *J Neurol Neurosurg Psychiatry* 2010; 81(4): 401–404.
24. Kutzelnigg A, Faber-Rod JC, Bauer J, et al. Widespread demyelination in the cerebellar cortex in multiple sclerosis. *Brain Pathol* 2007; 17(1): 38–44.
25. Herranz E, Hooker JM, Izquierdo-Garcia D, et al. Reply. *Ann Neurol* 2017; 81(2): 324–325.
26. Kutzelnigg A, Lucchinetti CF, Stadelmann C, et al. Cortical demyelination and diffuse white matter injury in multiple sclerosis. *Brain* 2005; 128(Pt. 11): 2705–2712.

27. Oh U, Fujita M, Ikonomidou VN, et al. Translocator protein PET imaging for glial activation in multiple sclerosis. *J Neuroimmune Pharmacol* 2011; 6(3): 354–361.

28. Magliozzi R, Howell OW, Reeves C, et al. A Gradient of neuronal loss and meningeal inflammation in multiple sclerosis. *Ann Neurol* 2010; 68(4): 477–493.

29. Deppe M, Tabelow K, Kramer J, et al. Evidence for early, non-lesional cerebellar damage in patients with multiple sclerosis: DTI measures correlate with disability, atrophy, and disease duration. *Mult Scler* 2016; 22(1): 73–84.

30. Valentino P, Cerasa A, Chiriaco C, et al. Cognitive deficits in multiple sclerosis patients with cerebellar symptoms. *Mult Scler* 2009; 15(7): 854–859.

31. Weier K, Penner IK, Magon S, et al. Cerebellar abnormalities contribute to disability including cognitive impairment in multiple sclerosis. *PLoS One* 2014; 9(1): e86916.

32. Tobyne SM, Ochoa WB, Bireley JD, et al. Cognitive impairment and the regional distribution of cerebellar lesions in multiple sclerosis. *Mult Scler* 2017; 24(13):1687–1695.

33. Prosperini L, Sbardella E, Raz E, et al. Multiple sclerosis: White and gray matter damage associated with balance deficit detected at static posturography. *Radiology* 2013; 268(1): 181–189.

34. Rizzo G, Veronese M, Tonietto M, et al. Generalization of endothelial modelling of TSPO PET imaging: Considerations on tracer affinities. *J Cereb Blood Flow Metab*. Epub ahead of print 1 January 2017. DOI: 10.1177/0271678X17742004.